

A Simplified 4-DOF Suspension Model for Dynamic Load/Unload Simulation and Its Application¹

Q. H. Zeng and D. B. Bogy
Computer Mechanics Laboratory
Department of Mechanical Engineering
University of California
Berkeley, CA 94720

Abstract

The mathematical models are critical for accurate simulation of the dynamic load/unload (L/UL) process in disk drives. The air bearing slider and the suspension are the most important parts in the L/UL mechanism. The air bearing modeling has been well researched, but an adequate and efficient suspension model is not available. A simplified 4-DOF suspension model is proposed in this paper. In this model the slider's pitch angle change due to the motion of the L/UL tab on the ramp is included in the simulation, and the forces applied by the ramp can be directly obtained. The effects of the suspension inertia are included in the effective inertia moments of the slider to improve the loading simulation. The model is implemented and applied to simulate the L/UL process of a pico slider that has been used in recent IBM mobile drives. The effects of the pitch static attitude (PSA), the roll static attitude (RSA), and some initial disturbances to the loading process are investigated. It is found that a positive PSA can significantly smooth the loading process. The effects of the PSA, the disk rpm, and the unload velocity on the unloading process are also simulated, and it is found that a positive PSA can also greatly improve the unloading performance of the slider. The results show that both the loading and unloading processes can be properly simulated by using the proposed model.

¹ This report has been submitted for publication in *ASME, Journal of Tribology*.

1 Introduction

Dynamic load/unload (L/UL) has been widely used in portable and removable drives, and it is beginning to appear in desktop and server drives as a way of avoiding slider-disk wear and stiction. In the implementation of the L/UL mechanisms, an important concern is the head-disk interface reliability. There are many experimental works available (Yamada and Bogy, 1988; Jeong and Bogy, 1992, 1993a; Levi and Talke, 1992; Fu and Bogy, 1994, 1995a, 1995b, 1996; Suk and Gillis, 1998). These works showed that the slider could be loaded onto the rotating disk without slider-disk contacts or without severe damage even with the contacts if the loading parameters and/or sliders were properly chosen. However, it is too difficult for engineers to design the mechanism using only experiments because there are too many design parameters of the mechanism, such as the L/UL parameters, slider air bearing designs, and suspension parameters. There are also many other difficulties in the experiments, such as the limitation of the capability of a given experimental system, and poor repeatability. Therefore, numerical simulation of the L/UL process is definitely required.

Jeong and Bogy (1993b) simulated a perpendicular L/UL mechanism. They studied the effects of the slider's loading velocity and initial pitch and roll on its dynamics during loading. They also investigated the contributions of the squeezing and shearing flows to the loading process, and obtained slider-disk contact criteria. Their research mainly focused on the loading process of positive pressure sliders. The unloading process causes no significant problems for positive pressure sliders, and therefore it was not considered important. However, negative pressure sliders are widely utilized in current drives because of their many advantageous features. Such features include faster take-off, less speed

sensitivity, better altitude insensitivity, less normal load sensitivity, smaller normal load (lower friction and wear during CSS) and lower flying height sensitivity to manufacturing tolerance. However, if negative pressure sliders are used in the L/UL system, the suction force may result in slider-disk contacts during the unload process. Therefore, Zeng, Chapin and Bogy (1998a), Hu, Jones and Li (1998) and Peng (1998) investigated the unload process of negative pressure sliders, and showed that the suction forces result in severe problems for most current sliders during unload. To prevent these problems, Zeng and Bogy (1998b) designed sliders specifically for L/UL applications, and achieved the preferred performance. To easily combine all of the design requirements, the industry currently employs another approach, specifically designed suspensions with limiters. Zeng and Bogy (1999) investigated the effects of the limiters on the dynamic L/UL process by numerical simulation, and found that the limiters significantly affect the unloading process.

The mathematical model is critical for properly simulating the L/UL process. All of these published works used a similar air bearing model, but they used quite different suspension models. In Jeong and Bogy's (1993b) simulation, the entire suspension was modeled by finite elements. This is a very comprehensive simulation. All effects of the suspension are included, but these effects can not be easily identified. Thus, it is inconvenient to apply it in the design process. Furthermore, it is very time consuming to calculate. In Hu et al's (1998) and Peng's (1998) simulation, the suspensions were modeled as three de-coupled springs and dampers, and the L/UL tab-ramp interactive was modeled by the "de-gramming" rate. The effects of suspensions are not sufficiently included in their simulations. In Zeng et al.'s (1998a and 1998b) simulation, the suspensions were modeled as three springs and dampers with varied parameters, and the

three degrees-of-freedom (DOFs) were de-coupled by defining offsets x_d and y_d in the X and Y directions. The L/UL tab-ramp interaction was modeled by moving the upper ends of the springs and dampers. Although the inertia effects of the suspensions were not included in the simulations, the calculated unloading process quantitatively matched well the experimental data (Zeng et. al., 1998a). The major advantages of this model are that not only are the suspension effects included, but also these effects can be easily identified. However, the effects of the slider's pitch change due to the movement of the L/UL tab are not included in this model. That has been found to significantly affect the loading process. Furthermore, the force applied on the ramp during the L/UL process is very important information for the L/UL mechanism design, and it cannot be obtained from this model.

In this paper, we propose another simplified suspension model for the L/UL simulation. The model has four DOFs. The slider's pitch changes due to the movement of the L/UL tab are included in the model, and the force applied by the ramp can be directly obtained from this model. The model is implemented and applied to simulate the L/UL process of a pico slider that was used in recent IBM mobile drives. The effects of the pitch static attitude (PSA), the roll static attitude (RSA), and the initial disturbances on the loading process are investigated, and it is found that a positive PSA can significantly smooth the loading process. The effects of the disk rpm, the unload speed, and the PSA on the unloading process are also simulated, and it is observed that a positive PSA can also greatly improve the unloading performance of the slider. The results show that both the loading and unloading processes can be accurately simulated by using the proposed model.

2 Mathematical Models

2.1 Slider Dynamics. Because of the constraints of the suspension, the slider's motion can be described as a system with three DOFs, as shown in Fig. 1, by the following governing equations

$$m \frac{d^2 z}{dt^2} = F_s + F_{ca} + F_{ci} + \iint_A (p - p_a) dA \quad (1)$$

$$I_\theta \frac{d^2 \theta}{dt^2} = M_{s\theta} + M_{ca\theta} + M_{ci\theta} + \iint_A (p - p_a)(x_0 - x) dA \quad (2)$$

$$I_\beta \frac{d^2 \beta}{dt^2} = M_{s\beta} + M_{ca\beta} + M_{ci\beta} + \iint_A (p - p_a)(y_0 - y) dA \quad (3)$$

In Eqs. (1)-(3), z , θ and β are the vertical displacement at the slider's center, and the slider's pitch and roll; m , I_θ and I_β are the mass and moments of inertia of the slider. F_{sz} is the suspension force in the Z-direction, $M_{s\theta}$ and $M_{s\beta}$ are suspension moments in the pitch and roll directions, p_a is the ambient pressure, and p is the air bearing pressure governed by the generalized Reynolds equation. If the air bearing clearance is less than the glide height, the asperity contact force and moments F_{ca} , $M_{ca\theta}$, and $M_{ca\beta}$ are calculated by the Greenwood-Williamson method (Hu, 1996). If the clearance is less than or equal to 0, the elastic-plastic model is used to approximately calculate F_{ci} , $M_{ci\theta}$, and $M_{ci\beta}$. The friction force F_f is also calculated, which has a contribution to the pitch and roll moments. In the limit of large disk Young's modulus, the results obtained here are similar to those obtained by the impulse-momentum method (Cha, 1993).

2.2 Suspension Model. The experimental results in (Fu and Bogy, 1995b) showed that radial acceleration does not significantly affect slider dynamics during ramp loading, so we ignored the effects of radial motion on the dynamics during the L/UL process. In an actual L/UL system, the suspension is actuated and excited by the airflow in the drive. The suspension dynamics can greatly affect the L/UL process. However, the negative pressure sliders can generate very stiff air bearings with resonance frequencies in the range from 40 kHz to 120 kHz for most 50% negative pressure sliders, and 80 kHz to 180 kHz for 30% sliders (Zeng and Bogy, 1998c). The suspension assemblies have much lower frequencies. Therefore, during times when the air bearing exists, the effects of the suspension on the slider can be simplified to its static load effects, i.e., the inertial effects of the suspension can be ignored. However, when the air bearing does not exist, as in the late stage of the unloading process or the early stage of the loading process, the initial effects of the suspension cannot be ignored. For simplicity, we include the effective inertia of the suspension in the slider inertial moments.

During the L/UL process, the contact conditions at the dimple, the limiter condition of the suspension, and the L/UL ramp point will change, causing the suspension to have several states. Typically, the integrated suspensions, such as the HTI 1650, have two states. One is the free state, in which there is no contact at the ramp. The other one has contact at the ramp. For the two-piece suspension such as the HTI 850, there are three states. In the first state, the dimple is closed and there is no contact at the ramp. In the second state, the dimple is still closed and the L/UL tab contacts the ramp. In the third state, the tab contacts the ramp and the dimple separates. The two-piece suspensions with limiters, such as those used in recent IBM mobile drives, have at least four states. In the fourth state, the tab

contacts the ramp, the dimple separates, and the limiters are engaged. In each state, the suspension has different parameters.

In the L/UL process, there are two forces and two moments applied on the suspension. One force, F_L , is applied on the L/UL tab in the vertical direction, and another is applied by the slider in the vertical direction. The slider also applies moments on the suspension in the pitch and roll directions. Then, one can obtain the displacements of the suspension at the L/UL tab and the slider's center, and rotations (pitch and roll) at the slider's center point as

$$\begin{Bmatrix} z_L \\ z \\ \theta \\ \beta \end{Bmatrix} = [H_j]_{4 \times 4} \begin{Bmatrix} -F_L \\ -F_S \\ -M_{s\theta} \\ -M_{s\beta} \end{Bmatrix} \quad (4)$$

where F_L is the force applied by the ramp, z_L is the displacement at L/UL tab. In each state j , the system has a different flexibility matrix $[H_j]$, which is calculated from the FE model of the suspension. Using these, and adding damping effects, we can obtain the force and moments applied on the slider center, and the force applied by the ramp as

$$\begin{Bmatrix} F_L \\ F_S \\ M_{s\theta} \\ M_{s\beta} \end{Bmatrix} = -[K_j]_{4 \times 4} \begin{Bmatrix} z_L \\ z \\ \theta \\ \beta \end{Bmatrix} - \begin{Bmatrix} 0 \\ c_z \dot{z} \\ c_\theta \dot{\theta} \\ c_\beta \dot{\beta} \end{Bmatrix} \quad (5)$$

where c_z, c_θ , and c_β are damping coefficients of the suspension in the vertical, pitch and roll directions. The ramp position z_R can be calculated by using equation

$$z_R = \frac{at^2}{2} + z_{R0}, \text{ if } t < v/a \quad (6)$$

or

$$z_R = v \left(t - \frac{v}{a} \right) + \frac{v^2}{2a} + z_{R0}, \text{ if } t \geq v/a \quad (7)$$

where a is the initial acceleration, v is the quickly reached steady L/UL velocity, and z_{R0} is the initial ramp height. If $z_L > z_R$ ($F_L = 0$), there is no contact at the ramp, and the suspension is in the free state. Then, Eq. (5) is modified to

$$\begin{Bmatrix} F_S \\ M_{s\theta} \\ M_{s\beta} \end{Bmatrix} = -[K_1]_{3 \times 3} \begin{Bmatrix} z \\ \theta \\ \beta \end{Bmatrix} - \begin{Bmatrix} c_z \dot{z} \\ c_\theta \dot{\theta} \\ c_\beta \dot{\beta} \end{Bmatrix} \quad (8)$$

In the free state, Eq. (4) is used to calculate z_L . If $z_L \leq z_R$, the system changes into the other state, and Eq. (5) is used to calculate the suspension force and moments.

2.3 Effective Inertia Moments of the Slider. Because the suspension inertia is ignored in the suspension models, its effects should be included in the slider inertia parameters, especially in the slider pitch and roll moments. The effective pitch and roll moments are

$$I_\theta = k_{\theta 1} / (2\pi f_\theta)^2 \quad (9)$$

$$I_\beta = k_{\beta 1} / (2\pi f_\beta)^2 \quad (10)$$

where $k_{\theta 1}$, and $k_{\beta 1}$ are the suspension stiffness in the pitch and roll directions in the free state, f_θ and f_β are the measured slider pitch and roll frequencies in the free state.

2.4 Numerical Solution. Substituting Eqs. (9), (10) and (5) or (8) into (1)-(3), and simultaneously solving the equations (1)-(3) and the generalized Reynolds equation, we can obtain the slider's response. For given slider attitudes (flying height, pitch and roll)

and L/UL tab movement, the four types of forces and moments are calculated. First is the asperity contact force and moments if the clearance is less than the glide height. Second is the impact force and moments if the clearance is less than zero. Next we solve the Reynolds equation to obtain the air pressure and thereby the air bearing force and moments. Finally we calculate the L/UL force, and the suspension force and moments by using Eq. (5) or (8). Then, substituting all of these force and moments into Eqs. (1)-(3), we solve the slider's equation of motion by using the Newmark method to find the new slider attitudes. If the new attitudes are close to the previous attitudes, the calculation in the one time step is finished. The time increment is properly selected based on the slider size, normal load, suspension stiffness, and L/UL velocity. For the 30% pico slider, we usually use a time increment between $0.5 \mu\text{s}$ and $0.05 \mu\text{s}$. If impacts occur, the time increment is decreased to 1% of the initial value. The CML Dynamic Load/Unload Simulator was developed to implement the model by updating the CML Air Bearing Dynamic Simulator (Chen and Bogy, 1998).

3 Applications

3.1 Suspension Parameters. A TSA suspension with limiters was modeled. The suspension is similar to the HTI 2030, but a L/UL tab and two limiters were added for the L/UL application. Assuming the two limiters, which are located at the two sides of the slider and nearby the slider's center, close or separate at some time, we can model the suspension with four states during the L/UL process. The accuracy of the suspension model parameters is critical for the L/UL simulation. The parameters that are required in the 4-DOF model cannot be directly measured, so we had to combine an experiment and

the FE analysis to obtain these parameters. First, the modal experiments of the suspension in the free state were carried out to obtain the modal frequencies and damping ratios of the first seven modes. The second and third modes are the slider pitch and roll modes that are very important for the L/UL simulation. These two modes should be very carefully measured. Second, a FE model was created, and the modal frequencies were calculated and compared with the experimental results. The FE model was modified to achieve good correlation between the analysis and experiment. Then, the stiffness matrices were calculated from the modified FE model. In each state, by sequentially applying a force at the L/UL tab, slider center in the Z direction, and pitch and roll moments, one can obtain the flexibility matrix by calculating the displacements at the point and the slider center in the Z direction, and the slider pitch and roll, respectively. Inverting the flexibility matrices, we obtained the stiffness matrices as shown in Table 1. Table 1 shows that the roll DOF is almost automatically de-coupled with the other three DOFs. The pitch DOF is coupled with the vertical displacement at the L/UL tab and slider center. Therefore, the L/UL tab motion on the ramp will result in the pitch change.

The slider's effective pitch and roll inertia moments calculated from Eqs. 9 and 10 are $6.15e-13 \text{ Nm}^2$ and $4.62e-13 \text{ Nm}^2$, respectively. The values calculated from the slider's density and dimensions are $2.21e-13 \text{ Nm}^2$ and $1.45e-13 \text{ Nm}^2$, respectively. We can see that the TSA gimbal significantly affects the slider dynamics. The damper coefficients were estimated from the slider's inertia and the measured modal frequencies and damping ratios of the first three modes.

3.2 Loading Process. A 30% pico slider that was used in recent IBM mobile drives is shown in Fig 2. The air bearing surface (ABS) parameters were measured from the samples. The L/UL performance of this slider attached to the 4-DOF model suspension is evaluated. The slider is loaded at the outer diameter of the 2.5 inch disk. In the base case, the disk rotational speed is 4500 RPM, the PSA and RSA are equal to zero, and the initial flying height is 50 μm . The initial loading velocity is zero, the acceleration is 100 m/s, and the vertical loading velocity is constant after it reaches 25.4 mm/s. The results for a typical loading process are shown in Figs. 3 and 4. Figure 3 shows the histories of the displacements at the L/UL tab (z_L) and the slider center (z), the minimum clearance between the disk and slider, and the slider roll and pitch. The minimum value of the minimum clearance in the loading process is about 26.38 nm. That means no contact occurs between the disk and the slider. The more detailed loading process is shown in the pitch and the air bearing force histories. The pitch history shows three stages. The initial pitch is about $-8 \mu\text{rad}$ although the PSA is equal to zero. This is because the initial L/UL height results in a change of the slider pitch. In the first stage, the pitch linearly increases from $-8 \mu\text{rad}$ to about $-3 \mu\text{rad}$ because of the L/UL tab movement, before the air bearing effects are encountered. Then, the pitch changes quickly because the air bearing quickly builds up. In the final stage, the slider gradually settles down. The force histories in Fig. 4 correspondingly show the three stages.

These results show that this slider incorporated with this suspension is smoothly loaded onto the disk and no contact occurs in the base case. However, the manufacture tolerances and various disturbances will affect the loading process in practical situations. Figure 5 a) shows a loading process, in which an initial disturbance is added in the slider pitch. The

disturbance is an initial pitch speed of 100 rad/s, which results in about 1 degree peak-to-peak oscillation in the pitch. This situation is likely to occur due to the excitation by the airflow and/or the L/UL movement. From Fig. 5 a), it can be observed that the slider contacts the disk (negative minimum clearance). We simulated many other cases, such as a -0.5 degree PSA, a -0.5 degree RSA, and an initial disturbance (100 rad/s) in the roll direction. In all of these cases, contacts occur between the slider and disk during the loading process. However, if a positive PSA is imposed, the loading process is significantly improved. Figure 6 shows a loading process, in which a 1.0 degree PSA is imposed, and same the initial disturbances in both pitch and roll are added. In this case, the slider doesn't contact the disk, and it can still be smoothly loaded on the disk.

3.2 Unloading Process. This slider has a relatively large negative pressure cavity, and it can generate a very stiff air bearing. Its resonance frequencies calculated by using the modal analysis method (Zeng et al., 1998c) are 92.77 kHz, 112.3 kHz and 161.1 kHz, respectively. Therefore, during times when the air bearing exists, many effects, such as suspension inertia, airflow disturbances, radial acceleration, can be ignored. Therefore, simulating the unloading process is easier and more accurate than simulating the loading process, because the air bearing exists most of the time in the unloading process, and the initial conditions are well defined. The unloading process is started at the steady flying state, while the air bearing is fully applied on the slider.

In the base case, the disk rotational speed is 4500 RPM, and the slider is unloaded at the outer diameter. The PSA and RSA are equal to zero, and the unloading velocity (vertical) is 127 mm/s. The results for an unloading process are shown in Figs. 7 and 8.

Figure 7 shows the histories of the L/UL force applied by the ramp, the air bearing force, the positive pressure force, the negative pressure force and the suspension force applied at the slider center. There are five stages in the unloading process. Figure 8 shows the displacement at the L/UL tab and the slider center, the minimum clearance, and the slider pitch and roll. When we evaluate the unloading performance of the slider, we mainly check if the slider contacts the disk, how much time is taken to finish the unloading process, how large are the forces applied by the ramp or on the ramp (ramp force). Contact may damage the media or result in a crash. A longer unloading time reduces the recordable area and/or requires a steeper L/UL ramp. A large ramp force increases the ramp wear and the actuator unloading torque. Therefore, no contact, a short unloading process and a small ramp force are preferred. The “lift-off” force, defined as the minimum air bearing force, is another very important indicator of the unloading performance. A large amplitude of lift-off force increases the ramp force, the unloading time, and the slider oscillation. From Figs. 7 and 8, it is observed that there is no slider/disk contact during the unloading process. The lift-off force is about 14.76 mN, and the maximum force applied by the ramp is about 37.46 mN. This slider has a large lift-off force that results in a strong slider oscillation and a large ramp force. The unloading process is finished in only about 1 ms because of the usage of the suspension limiters. Therefore, this slider can be properly unloaded by incorporating this suspension, but its unloading performance is not optimal.

Reducing the lift-off force is desired to improve the unloading performance of the slider. Therefore, the effects of the disk rotational speed, the unloading velocity and the PSA were simulated. Figure 9 a) shows the lift-off force with respect to the disk rotational speed. It is seen that a higher disk rpm gives a smaller lift-off force. That is mainly because

the slider has a larger pitch angle at a higher rpm, and a large pitch angle usually results in a smaller lift-off force. Figure 9 b) shows the lift-off force with respect to the unloading velocity. The trend is very clear; a smaller velocity gives a smaller lift-off force because of smaller squeeze effects of the air bearing. Figure 9 c) shows the effects of the PSA on the unloading process. We can see that the positive PSA significantly decreases the lift-off force. If the PSA has the value of 3° , the slider can be quickly and smoothly unloaded even without the limiters. The positive PSA increases the pitch angle in the steady flying state, and thereby results in the small lift-off forces. Therefore, the simulation results show that the unloading performance of the slider can be improved by decreasing the unloading velocity and/or applying a positive PSA. It is important to note that a positive PSA improves both the loading and unloading performance of the slider.

3.3 Comparison and Verification. The 3-DOF suspension model (Zeng et al., 1998a) and 1998b) was also used to simulate the L/UL process. The results show that we can obtain similar unloading simulation results and quite different loading simulation results by using both models. For example, in the base case of the unloading simulation, the lift-off forces calculated by the 3-DOF and 4-DOF models are 15.59 mN and 14.75 mN, respectively. The unloading simulation by using the 3-DOF model has been verified by experiments (Zeng et al., 1998a). Therefore, it is believed that both models are valid for the unloading simulation. Figure 5 b) shows the loading process calculated by using the 3-DOF model. Comparing Fig. 5 b) with Fig. 5 a), we can see that the results are quite different. The pitch change during loading significantly affects the loading process, but the pitch change due to the L/UL tab movement on the ramp is ignored in the 3-DOF model.

Therefore, in many cases, one can not use the 3-DOF model to properly simulate the loading process.

4 Conclusion

Numerically simulation of the dynamic L/UL process was investigated. A simplified 4-DOF suspension model is proposed to simulate the suspension effects on the L/UL process. In this model, the pitch change due to the L/UL tab movement on the ramp is included in the simulation, and the forces applied by the ramp can be directly obtained. The effect of the suspension inertia, which is very important for the pico slider and TSA suspensions, is included in the effective inertia moments of the slider. The model is successfully implemented and applied to simulate the L/UL process of a pico slider.

The L/UL process of a pico slider is investigated. The effects of PSA, RSA, and initial disturbances on the loading process are simulated, and it is found that a positive PSA can significantly smooth the loading process. The effects of the PSA, the disk rpm, the unload velocity on the unloading process were also calculated, and it is observed that a positive PSA can also greatly improve the unloading performance of the slider. The results show that both the loading and unloading processes can be properly simulated by using the proposed model.

Acknowledgments

This study is supported by the Computer Mechanics Laboratory at the University of California at Berkeley.

References

Cha, E., 1993, "Numerical Analysis of Head-Disk Assembly Dynamics for Shaped-Rail Sliders with Sub-Ambient Pressures Regions," Ph.D. Dissertation, Department of Mechanical Engineering, University of California, Berkeley.

Chen, L. S, and Bogy, D. B., 1998, "Air Bearing Dynamic Simulator User Manual V4.21," Technical Report No. 98-004, Computer Mechanics Laboratory, Department of Mechanical Engineering, University of California, Berkeley.

Fu, T. C., and Bogy, D. B., 1994, "Slider Vibrations induced by Ramp-Suspension Interaction During the Ramp Loading Process," *IEEE Transaction of Magnetics*, Vol. 30, No. 6, pp. 4170-4172.

Fu, T. C., and Bogy, D. B., 1995a, "Slider-Disk Contacts During the Loading Process in a Ramp-Load Magnetic Disk Drive," *ASME Advances in Information Storage Systems*, Vol. 6, pp. 41-54.

Fu, T. C., and Bogy, D. B., 1995b, "Drive Level Slider-Suspension Vibration Analysis and its Application to a Ramp-Load Magnetic Disk Drive," *IEEE Transaction of Magnetics*, Vol. 31, No. 6, pp. 3003-3005.

Fu, T. C., and Bogy, D. B., 1996, "Readback Signal Decrease Due to Dynamic Load Head-Disk Contacts," *ASME Journal of Tribology*, Vol. 118, pp. 370-375.

Hu, Y., 1996, "Head-Disk-Suspension Dynamics," Ph.D. Dissertation, Department of Mechanical Engineering, University of California, Berkeley.

Hu, Y., Jones, P. M., and Li, K., 1998, "Air Bearing Dynamics of Sub-Ambient Pressure Sliders During Dynamic Unload," ASME/STLE, International Tribology Conference, Toronto, Canada, Oct. 25-28.

Jeong, T. G., and Bogy, D. B., 1992, "An Experimental Study of the Parameters that Determine Slider-Disk Contacts During Dynamic Load-Unload," *ASME Journal of Tribology*, Vol. 114, No. 3, pp. 507-514.

Jeong, T. G., and Bogy, D. B., 1993a, "Dynamic Loading Impact Induced Demagnetization in Thin Film Media," *ASME Journal of Tribology*, Vol. 115, No. 3, pp. 370-375.

Jeong, T. G., and Bogy, D. B., 1993b, "Numerical Simulation of Dynamic Loading in Hard Disk Drives," *ASME Journal of Tribology*, Vol. 115, No. 3, pp. 307-375.

Levi, P. G., and Talke, F. E., 1992, "Load/Unload Investigations on a Rotary Actuator Disk Drive," *IEEE Transaction of Magnetics*, Vol. 28, No. 5, pp. 2877-2879.

Peng, J. P., 1998, "Theoretical Prediction of Ramp Loading/Unloading Process in Hard Disk Drives," ASME/STLE, International Tribology Conference, Toronto, Canada, Oct. 25-28.

Suk, M., and Gillis, D., 1998, "Effect of Slider Burnish on Disk damage During Dynamic Load/Unload," *ASME Journal of Tribology*, Vol. 120, Apr. pp. 332-338.

Yamada, T., and Bogy, D. B., 1988, "Load-Unload Slider Dynamics in Magnetic Disk Drives," *IEEE Transaction of Magnetics*, Vol. 24, No. 6, pp.2742-2744.

Zeng , Q. H., Chapin, M., and Bogy, D. B., 1998a, "Dynamics of the Unload Process for Negative Pressure Sliders," Asia-Pacific Magnetic Recording Conference, Singapore (APMRC), July 29-31, *IEEE Transaction of Magnetics* (in press).

Zeng , Q. H., and Bogy, D. B., 1998b, "Slider Air Bearing Designs for Load/Unload Applications," IEEE, The Magnetic Recording Conference (TMRC), Boulder, Colorado, Aug. 17-19, *IEEE Transaction of Magnetics* (in press).

Zeng , Q. H., and Bogy, D. B., 1998c, "Stiffness and Damping Evaluation of Air Bearing Sliders and New Designs with High Damping", *ASME Journal of Tribology* (in press)

Zeng , Q. H., and Bogy, D. B., 1999, "Effects of Suspension Limiters on the Dynamic Load/Unload Process: Numerical Simulation," Technical Report No. 99-002, Computer Mechanics Laboratory, Department of Mechanical Engineering, University of California, Berkeley, 1999.

Table 1 Suspension parameters

State j	Contact Conditions at			Stiffness matrices (N, m, rad)
	Ramp	Dimple	Limiters	
1	No	Yes	No	$1.465e+1$ $7.772e-3$ $-7.837e-6$ $7.772e-3$ $7.299e-5$ $-1.613e-8$ $-7.837e-6$ $-1.613e-8$ $7.049e-5$
2	Yes	Yes	No	$5.630e+2$ $-7.732e+2$ $-6.174e-3$ $1.927e-4$ $-7.732e+2$ $1.077e+3$ $1.625e-2$ $-2.725e-4$ $-6.174e-3$ $1.625e-2$ $7.306e-5$ $-1.824e-8$ $1.927e-4$ $-2.725e-4$ $-1.824e-8$ $7.049e-5$
3	Yes	No	No	$2.396e+1$ $-2.547e+1$ $-2.008e-2$ $3.322e-5$ $-2.547e+1$ $3.932e+1$ $3.552e-2$ $-5.128e-5$ $-2.008e-2$ $3.552e-2$ $7.244e-5$ $-2.121e-8$ $3.322e-5$ $-5.128e-5$ $-2.121e-8$ $7.049e-5$
4	Yes	No	Yes	$4.454e+2$ $-6.200e+2$ $-1.235e-1$ $6.071e-3$ $-6.200e+2$ $8.778e+2$ $1.814e-1$ $-8.378e-3$ $-1.235e-1$ $1.814e-1$ $9.800e-5$ $-1.703e-6$ $6.071e-3$ $-8.378e-3$ $-1.703e-6$ $5.644e-4$

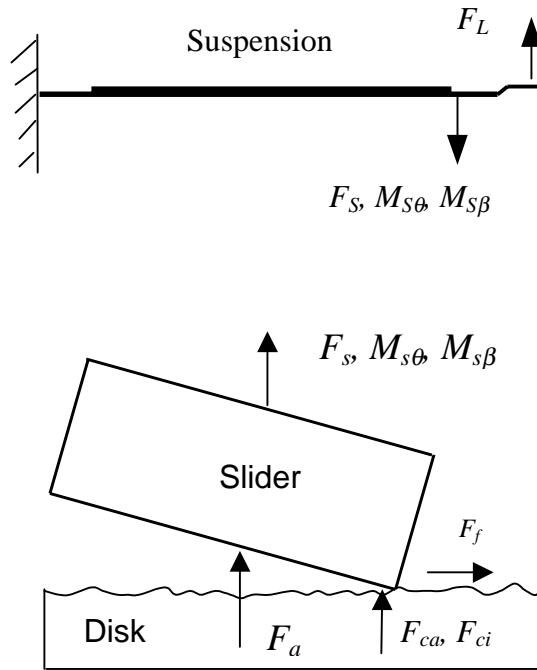


Fig. 1 Schematic drawing of the suspension and slider

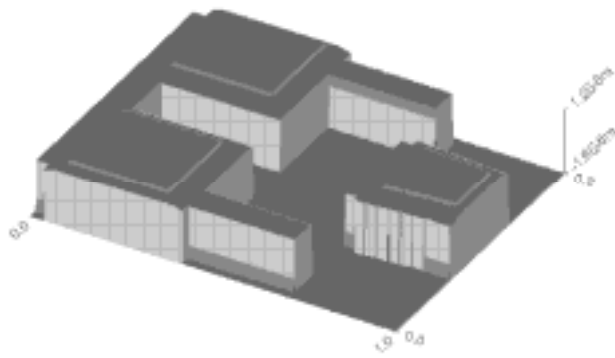
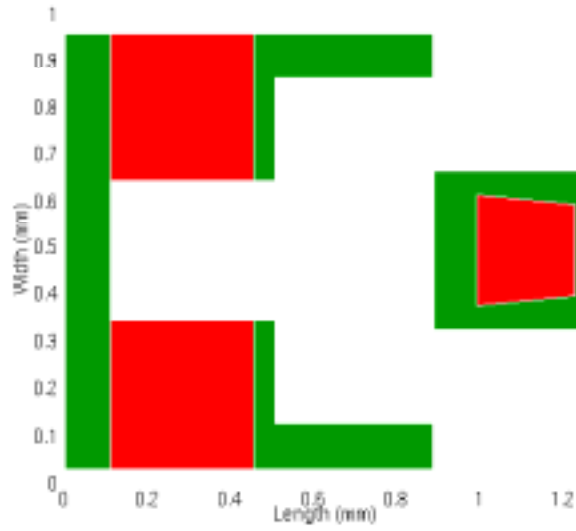


Fig. 2 An air bearing slider

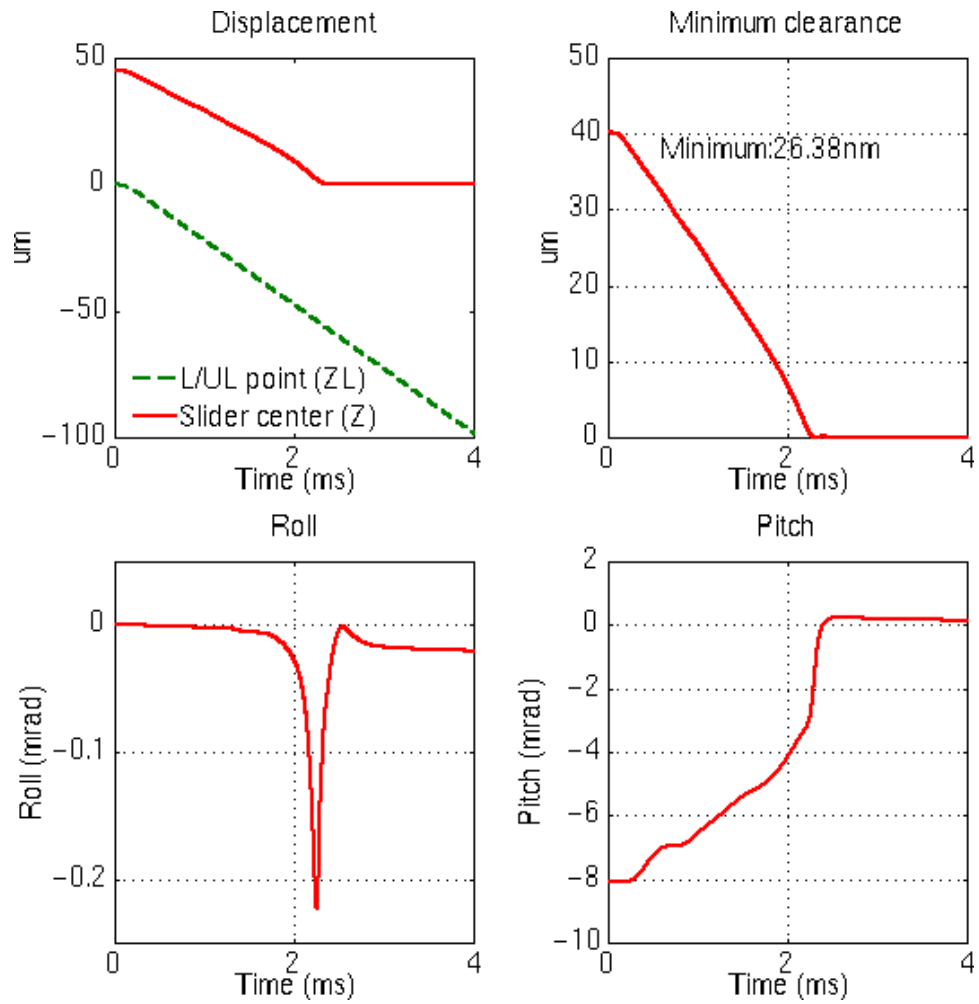


Fig. 3 Displacement at the L/UL point (tab) and slider attitudes during the loading process

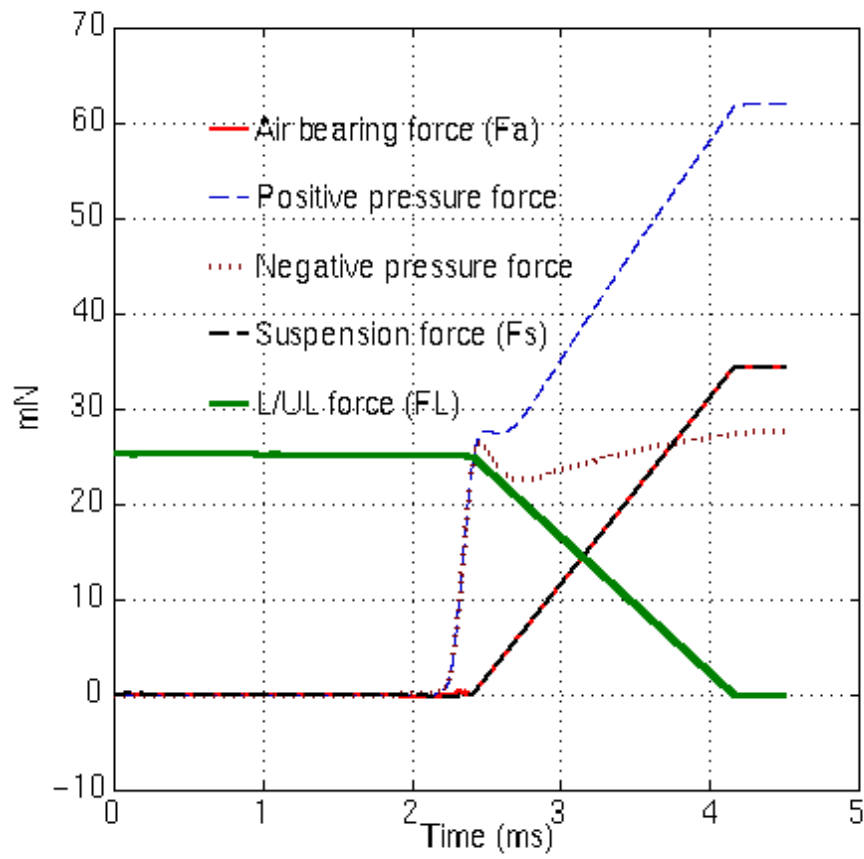
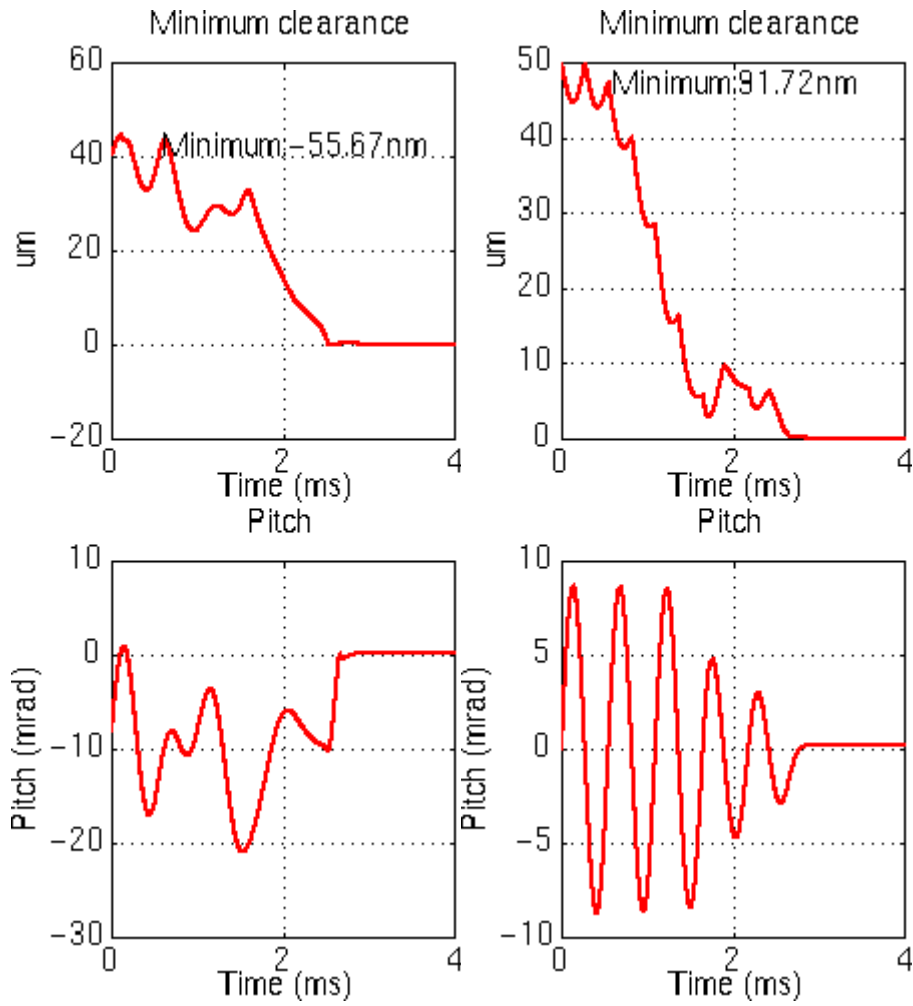


Fig. 4 Force histories during the loading process



a) 4-DOF model

b) 3-DOF model

Fig. 5 Minimum clearance and pitch histories of the slider during the loading process calculated by the different suspension models (a initial disturbance is included in the pitch direction)

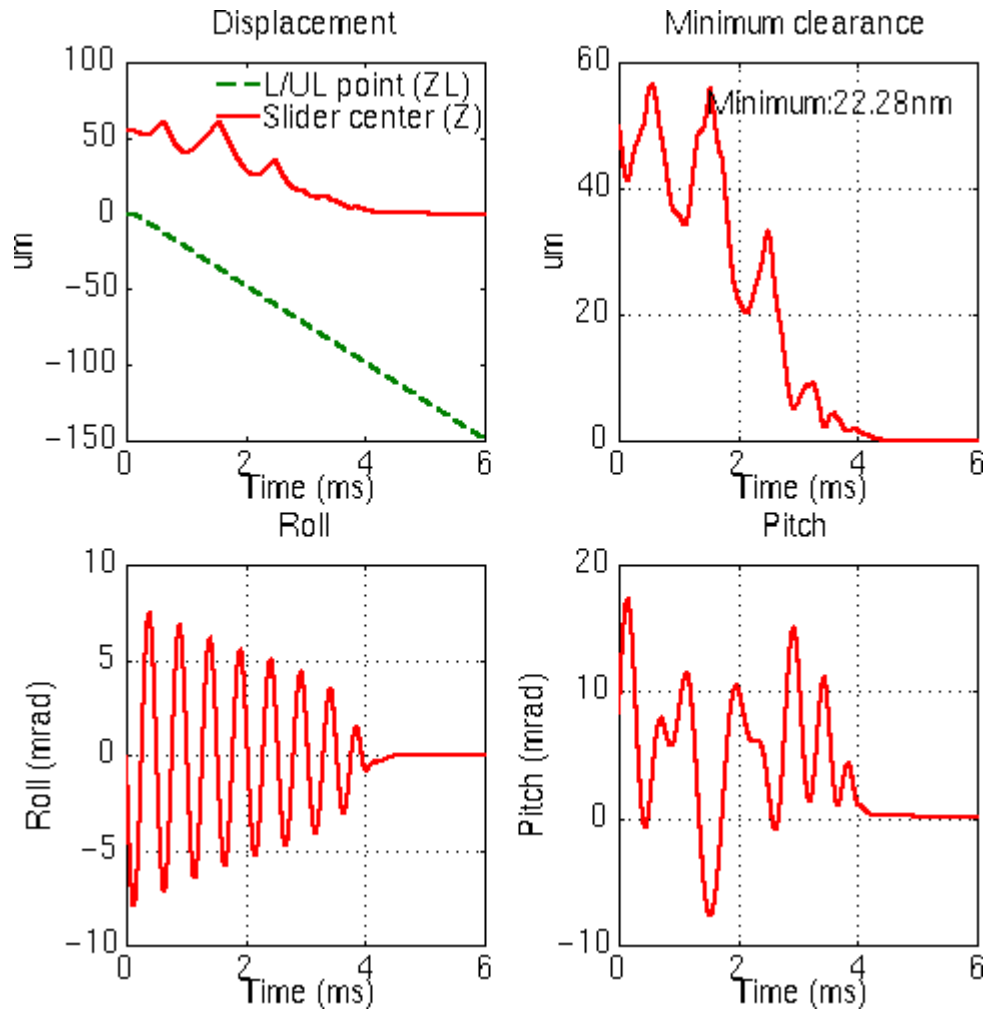


Fig. 6 Displacement at the L/UL point (tab) and slider attitudes during the loading process with a 1.0 degree PSA and initial disturbances (100 rad/s) in the pitch and roll directions

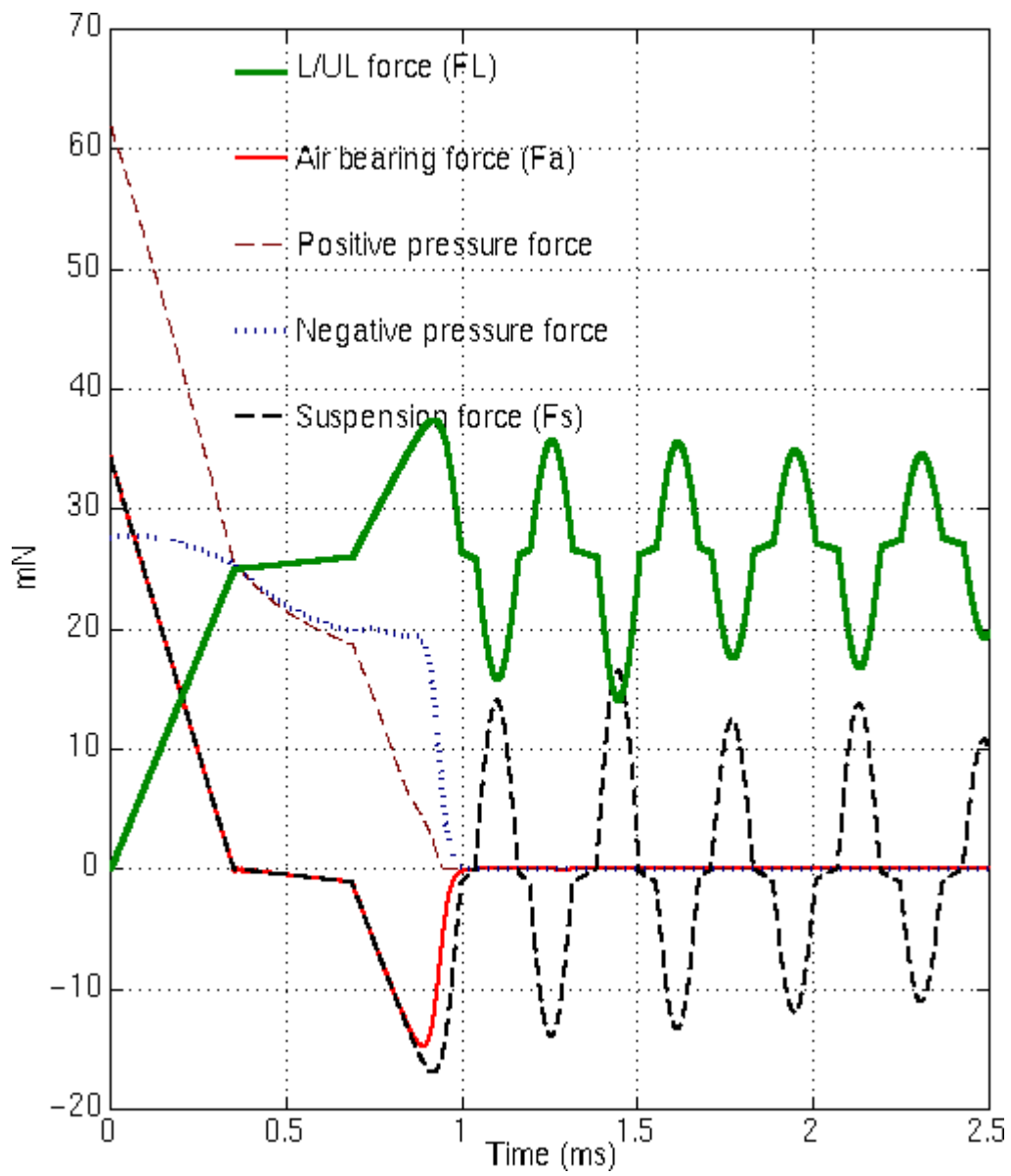


Fig. 7 Force histories during the unloading process

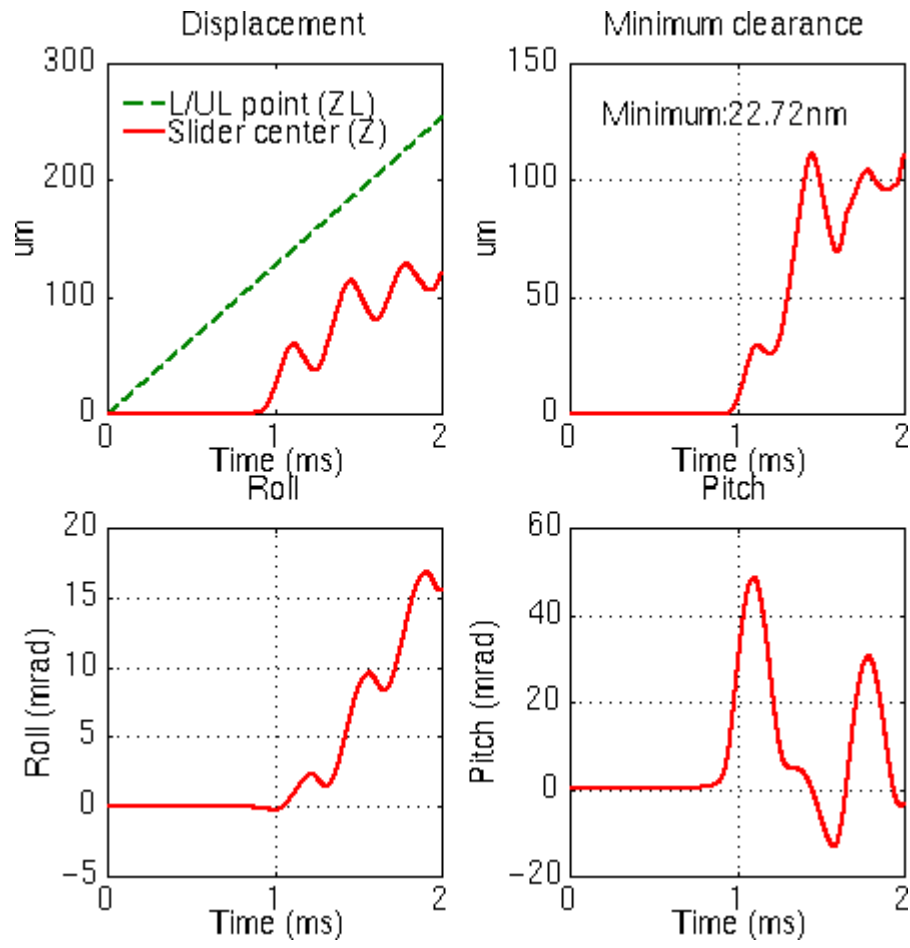


Fig. 8 Displacement at the L/UL point (tab) and slider attitudes during the unloading process

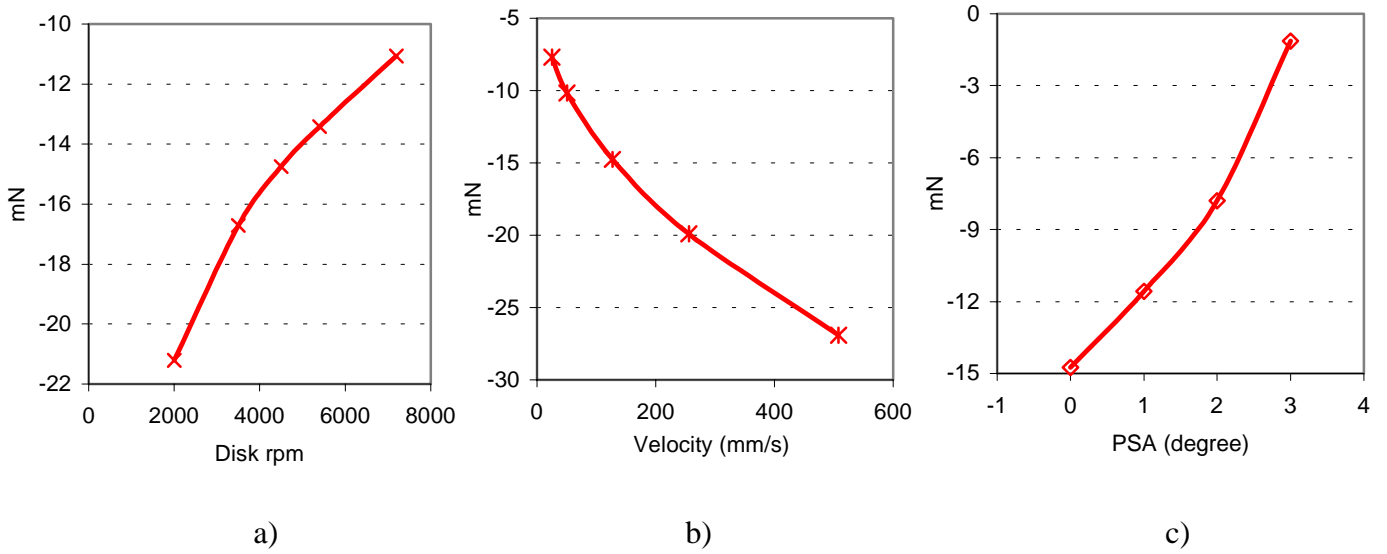


Fig. 9 Effects of the disk rpm, unloading velocity and PSA on the lift-off forces